

Mass Transfer Behavior of Phosphorus from the Liquid Slag Phase to Solid $2\text{CaO}\cdot\text{SiO}_2$ in the Multiphase Dephosphorization Slag



SENLIN XIE, WANLIN WANG, ZHICAN LUO, and DAOYUAN HUANG

The mass transfer behavior of phosphorus in the multiphase dephosphorization slag at 1623 K (1350 °C) is investigated in this article by adding the reagent P_2O_5 powders into the $\text{CaO}\text{-FeO}\text{-SiO}_2$ slag saturated with a directly precipitated $2\text{CaO}\cdot\text{SiO}_2$ phase. The results show that the phosphorus was first quickly dissolved and transferred from the liquid slag to the precipitated solid $2\text{CaO}\cdot\text{SiO}_2$ particle; then it reacted with the solid $2\text{CaO}\cdot\text{SiO}_2$ particle to form $(2\text{CaO}\cdot\text{SiO}_2\text{-}3\text{CaO}\cdot\text{P}_2\text{O}_5)$ solid solution at the edge of a large solid particle. The further diffusion of phosphorus from the formed $(2\text{CaO}\cdot\text{SiO}_2\text{-}3\text{CaO}\cdot\text{P}_2\text{O}_5)$ solid solution reaction layer into the core of the $2\text{CaO}\cdot\text{SiO}_2$ particle is the limiting step during the enrichment-phosphorus process. It is observed that the enrichment-phosphorus process is changed when the amount of added P_2O_5 content is increased and the formed solid solution phase is torn and peeled off from the surface of the $2\text{CaO}\cdot\text{SiO}_2$ particle. In addition, the study shows that the solid solution structure is changed and becomes more compacted with the addition of P_2O_5 content, leading to the increment of solid solution density.

DOI: 10.1007/s11663-016-0622-0

© The Minerals, Metals & Materials Society and ASM International 2016

I. INTRODUCTION

RECENTLY, to reduce the amount of steelmaking slag and increase the production of the low-phosphorus or ultra-low-phosphorus steel, a new refining method to improve the reaction efficiency of CaO by using a solid/liquid coexisting multiphase slag for hot metal efficient dephosphorization treatment was proposed.^[1] The research regarding the multiphase slag has been carried out intensively, and the formation mechanism of the $(2\text{CaO}\cdot\text{SiO}_2\text{-}3\text{CaO}\cdot\text{P}_2\text{O}_5)$ solid solution, the phosphorus distribution ratio between the $(2\text{CaO}\cdot\text{SiO}_2\text{-}3\text{CaO}\cdot\text{P}_2\text{O}_5)$ solid solution and the liquid phase, the phase relationship of the multiphase slag system under the different oxygen partial pressure, the free energies for the formation of $(2\text{CaO}\cdot\text{SiO}_2\text{-}3\text{CaO}\cdot\text{P}_2\text{O}_5)$ solid solution, as well as the activity of P_2O_5 in the $(2\text{CaO}\cdot\text{SiO}_2\text{-}3\text{CaO}\cdot\text{P}_2\text{O}_5)$ solid solution have been investigated.^[2–10]

It has been known that phosphorus dissolves into the molten $\text{CaO}\text{-FeO}\text{-SiO}_2$ slag system in the form of $3\text{CaO}\cdot\text{P}_2\text{O}_5$,^[11] and thus, it combines with $2\text{CaO}\cdot\text{SiO}_2$ solid phase to form $(2\text{CaO}\cdot\text{SiO}_2\text{-}3\text{CaO}\cdot\text{P}_2\text{O}_5)$ solid solution in basic oxygen furnace slag.^[12] To increase the efficiency of dephosphorization, it is very important to increase the mass transfer rate of phosphorus from the

liquid slag to the solid solution. It has been reported that there are two mechanisms for the mass transfer of phosphorus in the liquid multiphase slag,^[13] one is the direct precipitation mechanism, which occurs when the solid solution precipitates after the phosphorus is transferred from the hot metal to the liquid slag. Shimauchi *et al.*^[14] have clarified that the mass transfer rate *via* this mechanism is very fast as they found that the distribution ratio of phosphorus reaches the equilibrium condition irrespective of time at 1473 K (1200 °C). The other one is the diffusion mechanism, which happens when the $2\text{CaO}\cdot\text{SiO}_2$ phase precipitates first prior to the state that the phosphorus is transferred from hot metal to the liquid slag. Regarding the diffusion mechanism, several studies have been carried out.^[15–17] Inoue and Suito^[15] have found that the mass transfer of phosphorus from liquid $2\text{CaO}\cdot\text{SiO}_2$ saturated slag to the artificially prepared $2\text{CaO}\cdot\text{SiO}_2$ particles with 3 to 8 μm and formation of a uniform $(2\text{CaO}\cdot\text{SiO}_2\text{-}3\text{CaO}\cdot\text{P}_2\text{O}_5)$ solid solution is within 5 seconds, which indicates that the solid solution reaction is quick and the mass transfer rate by this mechanism is very high. Hoshikawa *et al.*^[16] have suggested that the dephosphorization rate is low when the artificially prepared $2\text{CaO}\cdot\text{SiO}_2$ powder is mixed with iron oxide to simulate the dephosphorization slag in the steelmaking process. In addition, Kitamura *et al.*^[17] have elaborated that the mass transfer of phosphorus between the $(2\text{CaO}\cdot\text{SiO}_2\text{-}3\text{CaO}\cdot\text{P}_2\text{O}_5)$ solid solution and the liquid slag is determined by the activity of phosphorus in the above-mentioned two phases, through dipping the artificially made $(2\text{CaO}\cdot\text{SiO}_2\text{-}3\text{CaO}\cdot\text{P}_2\text{O}_5)$ solid solution rod into the $(2\text{CaO}\cdot\text{SiO}_2\text{-}3\text{CaO}\cdot\text{P}_2\text{O}_5)$ saturated slag.

All these studies have assured that the occurrence of the mass transfer of phosphorus in the liquid slag and

SENLIN XIE, Graduate Student, and WANLIN WANG, Professor, are with the School of Metallurgy and Environment, Central South University, Changsha 410083, P.R. China. ZHICAN LUO, Graduate Student, and DAOYUAN HUANG, Lecturer, are with the International Research Center for Clean Metallurgy, Central South University, P.R. China. Contact e-mail: wanlin.wang@gmail.com

Manuscript submitted August 26, 2015.

Article published online March 4, 2016.

solid solution is complicated; however, having a clear understanding of the mass transfer of phosphorus in the multiphase slag, especially when it contains the directly precipitated crystal $2\text{CaO}\cdot\text{SiO}_2$ phase, is of extreme importance as it is directly related to the speed and efficiency of dephosphorization in the hot metal treatment. Therefore, the study of the mass transfer behavior of phosphorus in the solid $2\text{CaO}\cdot\text{SiO}_2$ and liquid slag coexisting multiphase slag system at the hot metal treatment temperature of 1623 K (1350 °C) is investigated in this article through the single hot thermocouple technique (SHTT) by adding the reagent P_2O_5 powders into the $\text{CaO}\text{-FeO}_t\text{-SiO}_2$ slag saturated with the directly precipitated $2\text{CaO}\cdot\text{SiO}_2$ phase.

II. EXPERIMENTAL APPARATUS AND PROCESS

A. Slag Sample Preparation

To obtain the $\text{CaO}\text{-FeO}_t\text{-SiO}_2$ slag saturated with the precipitated $2\text{CaO}\cdot\text{SiO}_2$ as the multiphase dephosphorization slag, the $\text{CaO}\text{-SiO}_2\text{-FeO}_t$ slag system with basicity of 1.5 was chosen for this work. The detailed chemical composition is given in Table I, which is marked in the ternary $\text{CaO}\text{-SiO}_2\text{-FeO}_t$ phase diagrams as shown in Figure 1, and it is located in the composition range saturated with dicalcium silicate ($2\text{CaO}\cdot\text{SiO}_2$).

To prepare the slag sample, the reagent grade CaCO_3 was first heated at 1223 K (950 °C) for 10 hours to obtain CaO. Then the well-mixed sample of CaO, SiO_2 , and FeC_2O_4 was premelted at 2073 K (1800 °C) in the induction furnace and quenched by water-cooled, sandwich-type Cu plates, where FeC_2O_4 was used as FeO_t as it would be decomposed into FeO_t .^[18] Finally the quenched slag was ground to 500 mesh by using a stainless-steel ball mill.

B. Experimental Apparatus

The SHTT was applied for the study of mass transfer of phosphorus in this article, and the details of SHTT apparatus have been described in the previous study.^[19–21] Its schematic figure is shown in Figure 2. The slag sample was mounted on a B-type thermocouple (0.5 mm, Pt-30 pct Rh, 6 pct Rh) and heated directly according to the temperature-controlling profile. Meanwhile, the real-time images of the slag sample were recorded directly by a connected camcorder through a high-temperature microscope for the *in situ* observation and analysis, and the corresponding temperature history could be obtained through the

temperature acquisition system. Thus, the crystallization process of various isothermals and nonisothermals could be carried out.

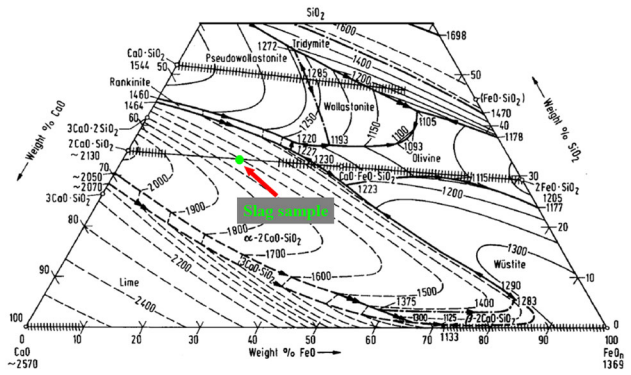


Fig. 1—The Composition of a slag sample in the $\text{CaO}\text{-SiO}_2\text{-FeO}_t$ phase diagrams.

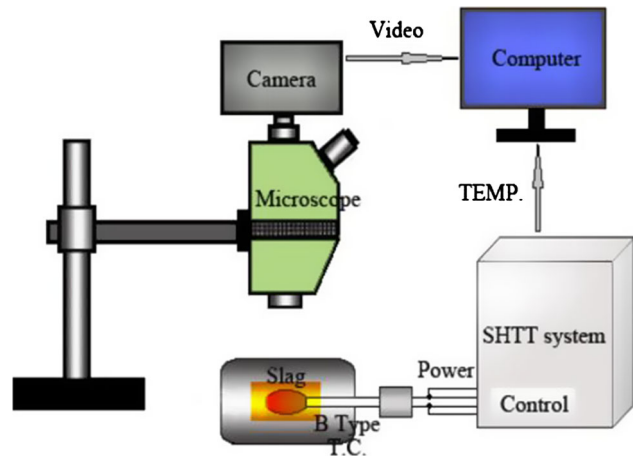


Fig. 2—Schematic figure of the hot thermocouple technique.

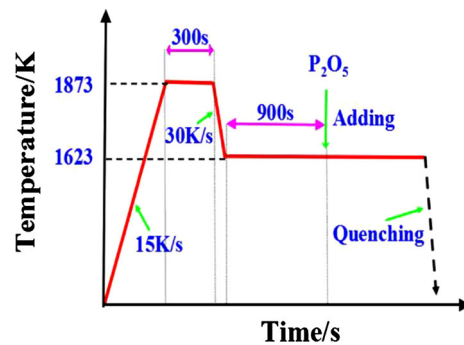


Fig. 3—Temperature-controlling profile for the experiment.

Table I. Chemical Composition of Slag Sample (Mass Pct)

Basicity $m(\text{CaO})/m(\text{SiO}_2)$	CaO	SiO_2	FeO_t	Total
1.5	48 pct	32 pct	20 pct	100 pct

C. Experimental Procedure

The tests were conducted according the temperature-controlling profile as shown in Figure 3. First the B-type thermocouple together with a certain amount of prepared sample powders was heated to 1873 K (1600 °C) at the rate of 15 K/seconds. Then it was held for 300 seconds to eliminate bubbles and homogenize its chemical composition. After that, it was cooled at the rate of 30 K/second to 1623 K (1350 °C) and held for 900 seconds to obtain the precipitation of the solid

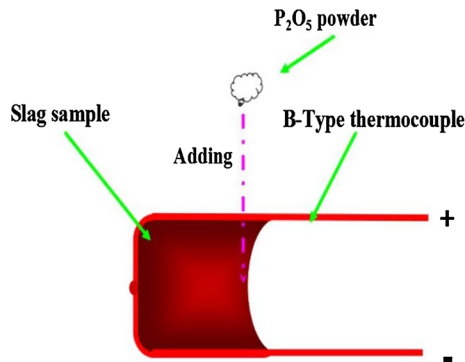


Fig. 4—Schematic drawing of adding P_2O_5 into the molten slag sample containing a precipitated $2CaO \cdot SiO_2$ solid phase.

$2CaO \cdot SiO_2$ phase. Then a certain amount of pure reagent P_2O_5 powders adhered to the Mo wire tip was added into the slag sample. The detailed process of adding P_2O_5 is shown in Figure 4. Thereafter, it was held for various times and quenched by turning off the power and flowing air with a flow rate of 1.5 L/minute simultaneously. Finally, the quenched slag sample was moved out from the B-type thermocouple and prepared according to the standard metallographic procedure for further scanning electron microscope (SEM) and energy-dispersive spectrometer (EDS) analysis.

III. RESULTS AND DISCUSSION

A. Identification of the Precipitated Crystal Phase in the $CaO-SiO_2-FeO_t$ Slag

To make sure that the precipitated crystal in the $CaO-SiO_2-FeO_t$ slag is $2CaO \cdot SiO_2$ phase, a 50-mg $CaO-SiO_2-FeO_t$ slag sample with basicity of 1.5 and 20 mass pct FeO_t was first heated to 1873 K (1600 °C). Then it was rapidly cooled to 1623 K (1350 °C) and held for 15 minutes; after that, it was quenched and subject to further analysis of SEM/EDS. The result is shown in Figure 5. From the point analysis results, combined with the linear scan, it was found that there are only three kinds of elements Ca, Si and O in the precipitated crystal, and the atom ratio of Ca to Si is very close to

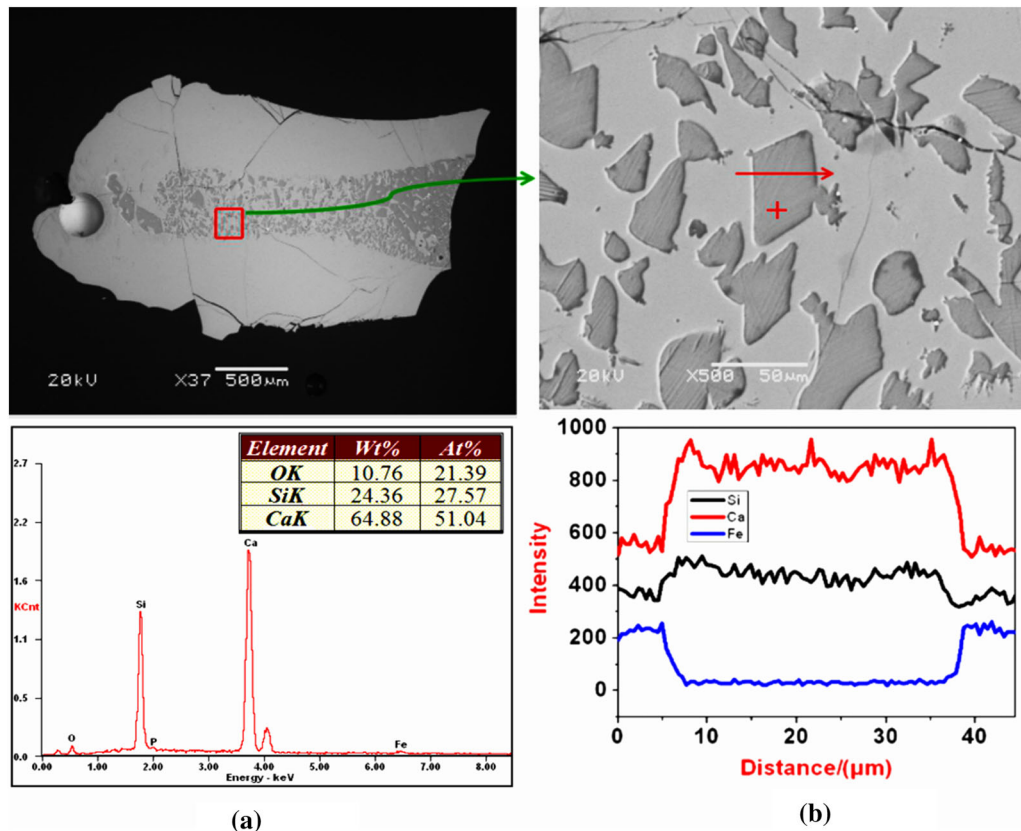


Fig. 5—SEM image and corresponding EDS results of the precipitated crystal in the quenched slag sample at 1623 K (1350 °C) held for 900 s: (a) point analysis and (b) line scan.

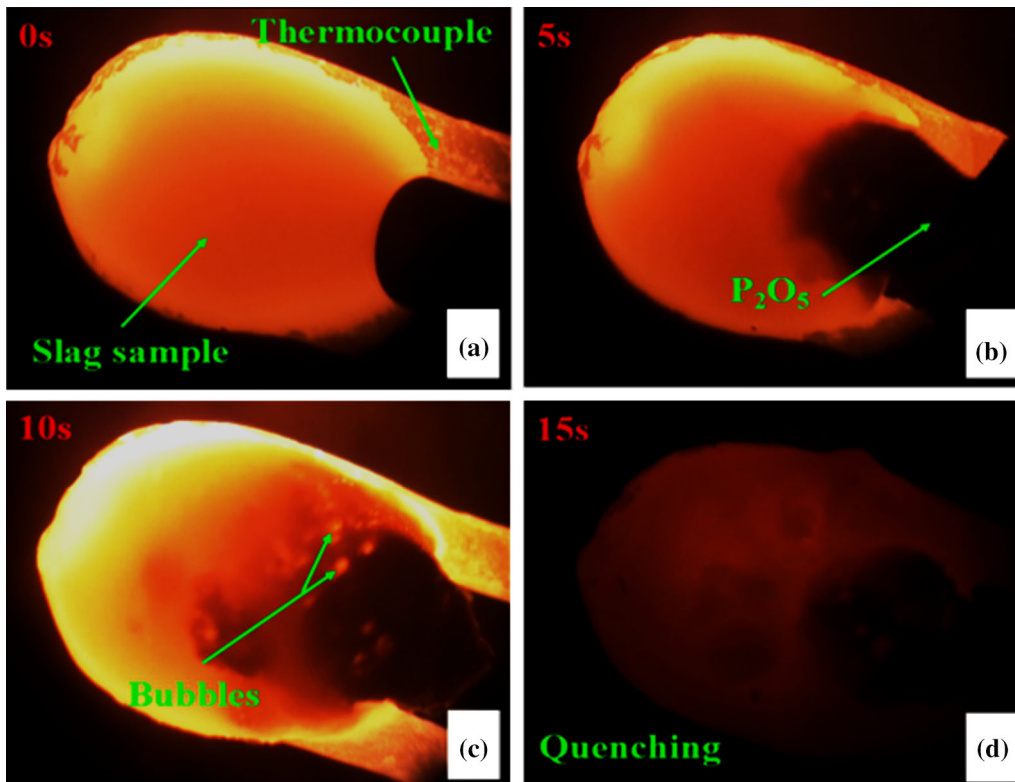


Fig. 6—Experimental process of adding P_2O_5 into the molten slag sample.

2.0, which indicated that the precipitated crystal in the slag sample is the $2CaO \cdot SiO_2$ phase. It is consistent with the composition of the slag sample in the ternary $CaO-SiO_2-FeO_t$ phase diagram. Furthermore, the crystallization ratio of $2CaO \cdot SiO_2$ was calculated through the image analyzer (Adobe Photoshop 7.0), which was defined as the fraction of crystallization area in the sample. The estimated value is about 35.38 pct, which is also consistent with the calculated result from the phase diagram based on the lever principle. The above results suggested that the crystallization of $2CaO \cdot SiO_2$ was almost finished during the isothermal crystallization process at 1623 K (1350 °C) within 15 minutes.

B. Observation of P_2O_5 Addition Process

To study the mass transfer behavior of phosphorous, 3.0-mg P_2O_5 powders were first added into the 50-mg molten $CaO-SiO_2-FeO_t$ slag saturated with precipitated $2CaO \cdot SiO_2$ and diffused for 15 seconds. Its process is shown in Figure 6, where the initial state of the slag sample at 1623 K (1350 °C) before the addition of P_2O_5 powder is illustrated in Figure 6(a). When P_2O_5 was added into the slag sample surface from the right side, the P_2O_5 powders were observed to dissolve immediately in the molten slag and diffuse into the center of the molten slag to combine/react with the precipitated $2CaO \cdot SiO_2$ crystal phase. Meanwhile, the generation of bubbles was observed due to the violent interaction and the evaporation of P_2O_5 , which can be observed in Figure 6(c). Then, the slag sample was

cooled at 15 seconds by turning off the power and flowing air simultaneously as shown in Figure 6(d). Finally the cross section of slag sample was analyzed through SEM/EDS after it was moved out from B-type thermocouple and prepared for the standard metallographic procedure.

The SEM image of the slag sample combined with the corresponding EDS of the crystals are shown in Figure 7, and the results indicate there are two different types of solid phases appearing around the P_2O_5 addition zone. According to EDS results, the white crystal-1 was identified as the high FeO_t containing phase, while the gray crystal-2 was suggested as the $3CaO \cdot P_2O_5$ phase. When P_2O_5 dissolves in the molten slag, it would prefer to form the $3CaO \cdot P_2O_5$ phase as it has the minimum Gibbs free energy of formation among the calcium phosphates in the current system, which causes the concentration of FeO_t in this zone to be relatively increased; thus, the iron oxide-rich phase is precipitated.

C. Determination of the Limiting Step of the Mass Transfer of Phosphorus

The tests of adding 3.0-mg P_2O_5 powder into the 50-mg $CaO-SiO_2-FeO_t$ slag saturated with the directly crystallized $2CaO \cdot SiO_2$ for different holding times, such as 15, 60, 300, 600, and 900 seconds, have been conducted at 1623 K (1350 °C), and the element mapping of P, Ca, and Fe for each slag sample is shown in Figure 8, respectively. It was found that the

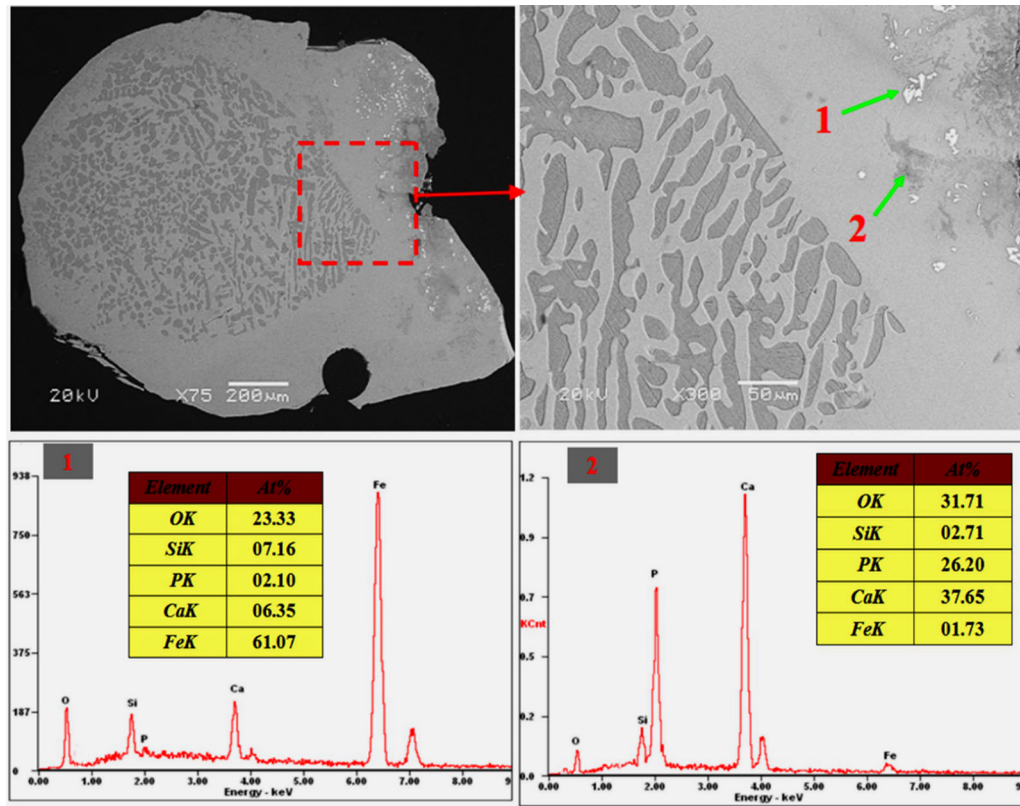


Fig. 7—SEM image of the sample being treated for 15 s and the corresponding EDS results of crystal-1 and crystal-2.

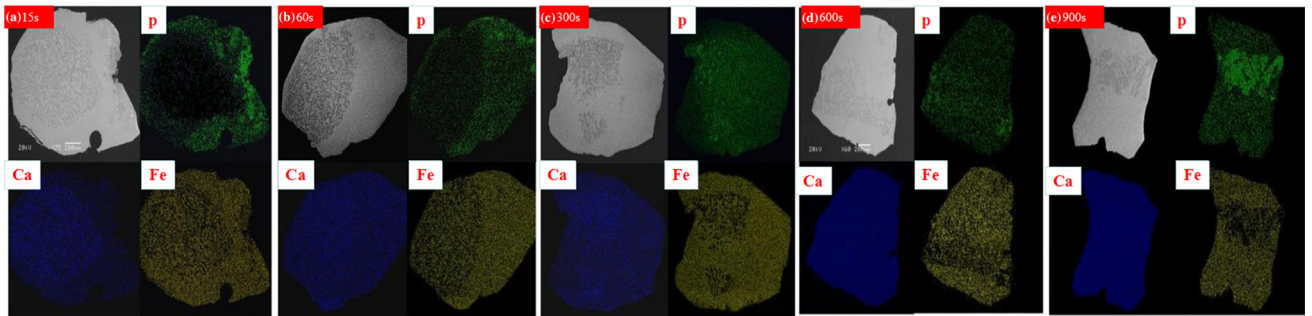


Fig. 8—Global SEM images and the corresponding element P, Ca, and Fe mapping of each slag sample after adding P_2O_5 for different holding times (a) 15 s, (b) 60 s, (c) 300 s, (d) 600 s, and (e) 900 s.

concentration of element Ca is much concentrated in the crystal-enriched zone when the holding time is 15 seconds, while the corresponding concentration of element Fe shows the opposite results, as the element Fe was the impurity components in the crystal phase. The gray zone was identified as the precipitated solid $2CaO \cdot SiO_2$ phase according to the earlier reported results. For the element P, it was found that within 15 seconds, the phosphorus was concentrated in the right side of the adding area and began to diffuse to the left-side liquid phase. However, it is very hard to find the P element in the precipitated solid $2CaO \cdot SiO_2$ phase zone as shown in Figure 8(a). When the holding time reaches 60 seconds, it is observed that the distribution of element P in the liquid phase

becomes more uniform external of the crystal phase as illustrated in Figure 8(b) and that Ca and Fe show the similar distribution of Figure 8(a). When the diffusion time goes to 300 seconds, the concentration of element P in the precipitated solid $2CaO \cdot SiO_2$ phase zone increases at the edge of the crystals as shown in Figure 8(c) indicating the formation of $(2CaO \cdot SiO_2 - 3CaO \cdot P_2O_5)$ solid solution. The concentration of P continuously increases and diffuses to the center of the crystals with the extension of holding time, which indicates that there would be more P-containing solid solution formed in the original $2CaO \cdot SiO_2$ phase as shown in Figures 8(d) through (e). Those results implied that the mass transfer of phosphorus in the liquid phase is faster than that in

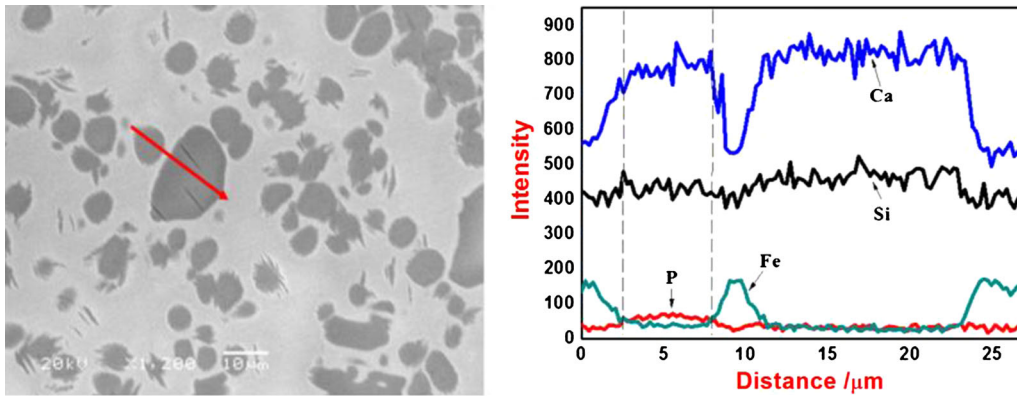


Fig. 9—SEM image and line scan of the crystallized $2\text{CaO}\cdot\text{SiO}_2$ in the slag sample being treated for 300 s.

the solid $2\text{CaO}\cdot\text{SiO}_2$ phase; in other words, the mass transfer of phosphorus in the solid $2\text{CaO}\cdot\text{SiO}_2$ phase is the limiting step of phosphorus mass transfer, which is consistent with study of Inoue and Suito.^[15]

D. SEM/EDS Analysis of the Solid Particles

To elaborate on the detailed mass transfer behavior of phosphorus in the solid $2\text{CaO}\cdot\text{SiO}_2$ phase, the slag sample held for 300 seconds in the above test was detected by SEM/EDS as shown in Figure 9. From its corresponding linear scan result, it is clear that the both elements Ca and Si show similar intensity for small and large solid particles, but the intensity of the P element is higher in the small size particle (less than $10\ \mu\text{m}$), which suggests the formation of $(2\text{CaO}\cdot\text{SiO}_2\text{-}3\text{CaO}\cdot\text{P}_2\text{O}_5)$ solid solution would easily occur in small particles. The reason is that the small particle has a relatively large specific surface area in comparison with the large particles; thus, the driving force for P penetration increases.

To elaborate on the phosphorus distribution in the large $2\text{CaO}\cdot\text{SiO}_2$ particle, the large size particle with $50\ \mu\text{m}$ in the sample held for 600 seconds was analyzed with SEM, and the corresponding EDS results at the different locations are shown in Figure 10. It is demonstrated that only the rim part of the solid $2\text{CaO}\cdot\text{SiO}_2$ particle has been changed to the $(2\text{CaO}\cdot\text{SiO}_2\text{-}3\text{CaO}\cdot\text{P}_2\text{O}_5)$ solid solution, while the inside core part is kept as the $2\text{CaO}\cdot\text{SiO}_2$ phase. Furthermore, there is a concentration gradient of phosphorus that occurred from the $(2\text{CaO}\cdot\text{SiO}_2\text{-}3\text{CaO}\cdot\text{P}_2\text{O}_5)$ solid solution reaction layer to the inside core of the solid particle. The current results indicated that the size of the $2\text{CaO}\cdot\text{SiO}_2$ particle has a significant impact on the efficiency of dephosphorization when the solid $2\text{CaO}\cdot\text{SiO}_2$ /liquid phase coexisting multiphase slag was used for the hot metal treatment, which is a good topic for further study.

E. Diffusion Mechanism of Phosphorus in the Multiphase Slag

Based on the above results in this study, it could be concluded that the mass transfer of phosphorus in the multiphase slag is limited in the large solid $2\text{CaO}\cdot\text{SiO}_2$ phase. Figure 11 shows the schematic diffusion

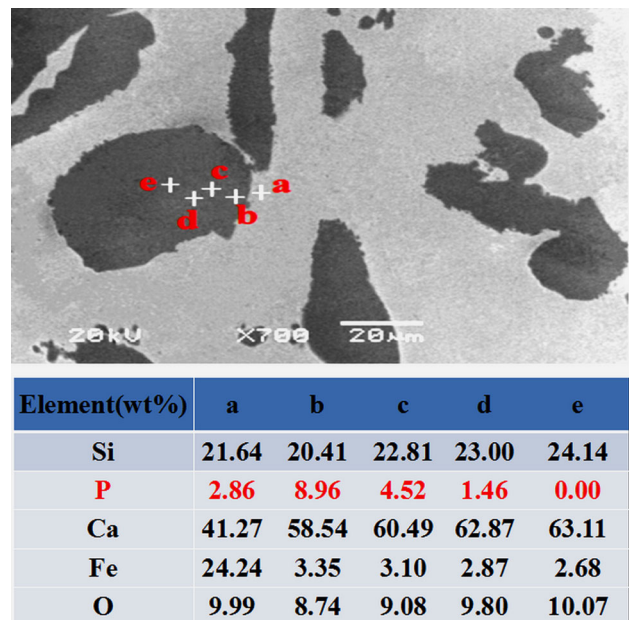


Fig. 10—SEM image and the corresponding EDS results of the sample that being treated for 600 s.

mechanism of phosphorus in the multiphase slag containing precipitated $2\text{CaO}\cdot\text{SiO}_2$, where the dissolved phosphorus first diffused from the liquid phase to the precipitated $2\text{CaO}\cdot\text{SiO}_2$ particle surface; then it reacted with $2\text{CaO}\cdot\text{SiO}_2$ and formed the $(2\text{CaO}\cdot\text{SiO}_2\text{-}3\text{CaO}\cdot\text{P}_2\text{O}_5)$ solid solution reaction layer; thereafter, the phosphorus diffused through the $(2\text{CaO}\cdot\text{SiO}_2\text{-}3\text{CaO}\cdot\text{P}_2\text{O}_5)$ solid solution reaction layer and continued to react with $2\text{CaO}\cdot\text{SiO}_2$, so the $(2\text{CaO}\cdot\text{SiO}_2\text{-}3\text{CaO}\cdot\text{P}_2\text{O}_5)$ solid solution reaction layer would gradually expand with the extension of time. Finally the whole solid $2\text{CaO}\cdot\text{SiO}_2$ phase was changed to the $(2\text{CaO}\cdot\text{SiO}_2\text{-}3\text{CaO}\cdot\text{P}_2\text{O}_5)$ solid solution gradually. Thus, the phosphorus was enriched in the precipitated $2\text{CaO}\cdot\text{SiO}_2$ particles to achieve dephosphorization.

F. Clarification of the Peeling Phenomenon

A similar experiment was carried out under the same condition by adding more ($6.0\ \text{mg}$) P_2O_5 powders into

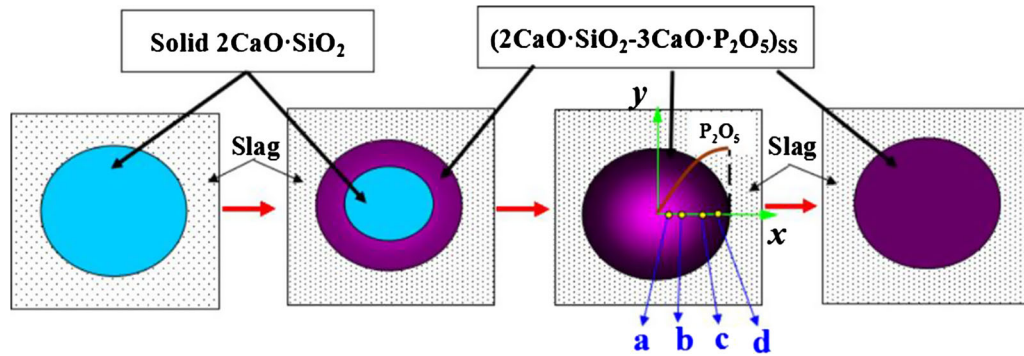


Fig. 11—Schematic of diffusion mechanism in solid $2\text{CaO}\cdot\text{SiO}_2$ phase.

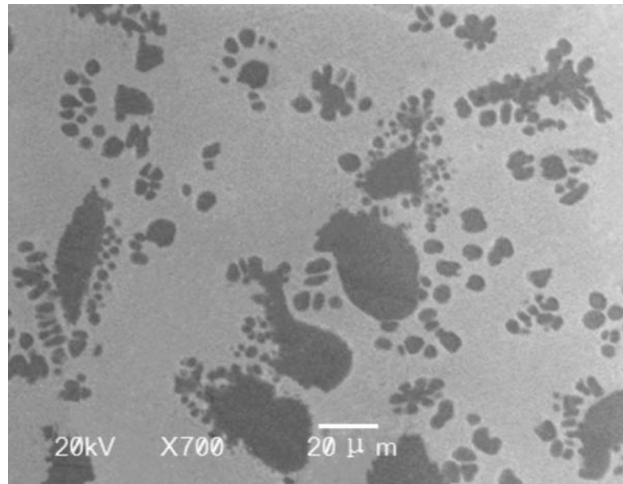


Fig. 12—Partial cross section of SEM image for the sample slag being treated for 15 s.

the 50-mg $\text{CaO}\cdot\text{SiO}_2\text{-FeO}_t$ slag saturated with the directly crystallized $2\text{CaO}\cdot\text{SiO}_2$ phase. An interesting phenomenon was then observed in the slag samples at the different holding times. The partial cross-section SEM image of the slag sample at the holding time of 15 seconds was chosen as a representative and is shown in Figure 12. It can be seen that many small particles were scattering around the large particles with the size larger than $20\ \mu\text{m}$. To clarify this phenomenon, the slag sample at the holding time of 30 seconds was detected by SEM/EDS carefully; the SEM image and the corresponding linear scan results are illustrated in Figure 13. It was observed that a series of small solid particles with 5 to $10\ \mu\text{m}$ were scattering around the surface of a large solid particle. The chemical composition of the small ones was identified as $(2\text{CaO}\cdot\text{SiO}_2\text{-}3\text{CaO}\cdot\text{P}_2\text{O}_5)$ solid solution, while the large solid particle was recognized as the crystallized $2\text{CaO}\cdot\text{SiO}_2$ phase. This situation in the present work was called the peeling phenomenon, in which the phosphorus first react with the external part of the large particle, and then the formed solid solution is broken away from the original large particle. Finally the formed solid solution phases scatter around the surface of the large particle.

The possible steps for the observed phenomenon is proposed as shown in Figure 14. First the phosphorus in the liquid slag penetrates into the surface of a $2\text{CaO}\cdot\text{SiO}_2$ particle and rapidly forms the $(2\text{CaO}\cdot\text{SiO}_2\text{-}3\text{CaO}\cdot\text{P}_2\text{O}_5)$ solid solution reaction layer. Then the $(2\text{CaO}\cdot\text{SiO}_2\text{-}3\text{CaO}\cdot\text{P}_2\text{O}_5)$ solid solution reaction layer is torn from the original phase; finally the $(2\text{CaO}\cdot\text{SiO}_2\text{-}3\text{CaO}\cdot\text{P}_2\text{O}_5)$ solid solution reaction layer is peeled off from the surface of the $2\text{CaO}\cdot\text{SiO}_2$ particle.

G. Investigation of the Structure and Density of the Solid Solution with Various P_2O_5

In the present work, to illustrate further the mass transfer behavior of phosphorus, the structure and density of the solid solution $(2\text{CaO}\cdot\text{SiO}_2\text{-}3\text{CaO}\cdot\text{P}_2\text{O}_5)$ solid solution containing different P_2O_5 content was investigated. The P_2O_5 content in the $(2\text{CaO}\cdot\text{SiO}_2\text{-}3\text{CaO}\cdot\text{P}_2\text{O}_5)$ solid solution was designed from 5 to 20 mass pct at an interval of 5 mass pct. The detailed chemical composition of samples is shown in Table 2.

The phase diagram of $2\text{CaO}\cdot\text{SiO}_2\text{-}3\text{CaO}\cdot\text{P}_2\text{O}_5$ with different P_2O_5 content is given in Figure 15.^[9] First, different amounts of reagent-grade chemicals of CaCO_3 , SiO_2 , and $(\text{NH}_4)_2\text{HPO}_4$ were prepared and well mixed according to Table 2. Then they were melted at 1773 K ($1500\ ^\circ\text{C}$) for 10 hours and quenched in the air to obtain the $(2\text{CaO}\cdot\text{SiO}_2\text{-}3\text{CaO}\cdot\text{P}_2\text{O}_5)$ solid solution with various P_2O_5 content.^[22] Thereafter, part of them were crushed and ground into powders for X-ray energy-dispersive spectroscopy (XRD) tests by using Cu K α radiation ($1.54184\ \text{\AA}$) in a range of $2\theta = 10$ to $80\ \text{deg}$ with a step size of $4\ \text{deg/second}$, and the results are shown in Figure 16. Meanwhile, some powders were tested by the infrared spectroscopy (Nicolet-6700), and the results are presented in Figure 17. In addition, the density of each sample was detected through the true density analyzer (3H-2000TD) as illustrated in Figure 18.^[23] Finally, their cross sections were observed through the SEM under the same magnification, which is displayed in Figure 19.

It can be seen from Figure 16 that the difference between the $(2\text{CaO}\cdot\text{SiO}_2\text{-}3\text{CaO}\cdot\text{P}_2\text{O}_5)$ solid solutions containing various P_2O_5 is the intensity of the main characteristic peaks, where the intensity was increased at

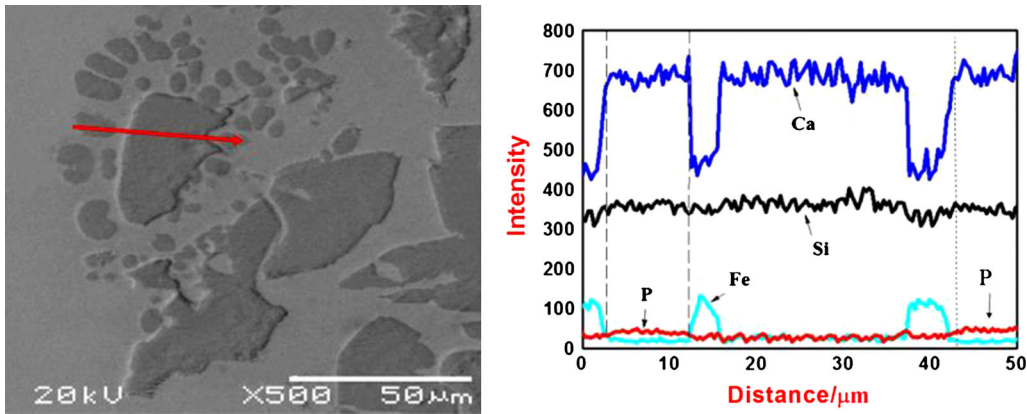


Fig. 13—SEM image and line scan of the crystallized phases in the slag sample being treated for 30 s.

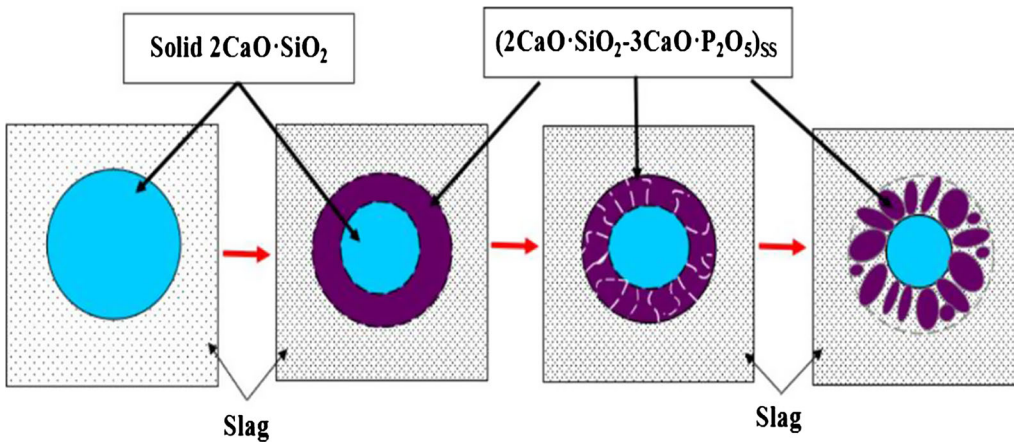


Fig. 14—Schematic diagram of the peeling phenomenon for the solid solution.

Table II. Chemical Composition of Solid Solution Containing Different P₂O₅ Content (Mass Pct)

P ₂ O ₅ Content (Pct)	Solid Solution		
	2CaO·SiO ₂ (Pct)	3CaO·P ₂ O ₅ (Pct)	Total (Pct)
5	89.085	10.915	100
10	78.169	21.831	100
15	67.254	32.746	100
20	56.338	43.662	100

the degree of $2\theta = 32.4$, while it was reduced at the degree of $2\theta = 31.7$, with the increment of P₂O₅ content; in addition, some peaks shifted and some small peaks disappeared, which indicates that the lattice constant was changed with the change of P₂O₅ content. There is no standard XRD patterns for the (2CaO·SiO₂-3CaO·P₂O₅) solid solution containing different P₂O₅ content as it is the infinite solid solution; therefore, it was determined that the structure of the solid solution containing 5 and 10 mass pct P₂O₅ content is highly similar to that of the α -Ca₂SiO₄ (JCPDS NO. 86-0399),^[22] while the solid solution containing 15 and 20 mass pct P₂O₅ content is the same as the

α -Ca₂SiO₄(JCPDS NO.86-0401),^[24] which suggests that the structure of the (2CaO·SiO₂-3CaO·P₂O₅) solid solution was varied with P₂O₅ content. From Figure 17, it is obvious that the IR spectra can be separated into two bands. The first band is in the 1200 to 800 cm⁻¹ range that has been generally assigned to the symmetric stretching vibration of SiO₄ tetrahedral^[25,26] and PO₄ groups,^[27-29] while the second band is in the range of 600 to 400 cm⁻¹ that generally has been represented as bending vibration of T-O-T, where T refers to Si or P elements.^[27,30] It was found that the first band become more intensive and wide with the increment of P₂O₅ content, which suggests there would be more 3CaO·P₂O₅ phase formed in the solid solution. In addition, a peak that associated with the bending vibration (ν_4) of P-O-P appeared in the second band and it became stronger with the addition of P₂O₅ content as shown in the sample with 15 and 20 pct P₂O₅.^[27,31] The current results also confirmed that the structure of the (2CaO·SiO₂-3CaO·P₂O₅) solid solution was changed with the increase of P₂O₅. It has been acknowledged that the variation of the crystal structure will eventually lead to a change in density, and the density of the above solid solution samples is shown in the Figure 18. It is obvious that the density of the solid solutions was increased gradually with the increment of P₂O₅ content.

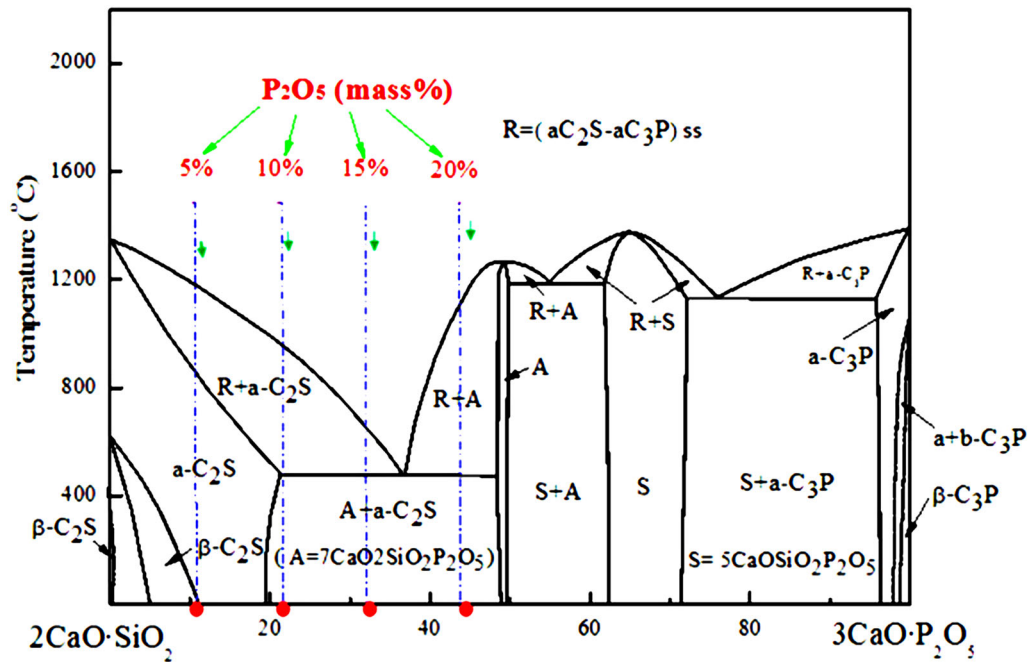


Fig. 15—Chemical composition of the solid solution with various P_2O_5 content in the $(2CaO \cdot SiO_2 - 3CaO \cdot P_2O_5)$ phase diagram.^[9]

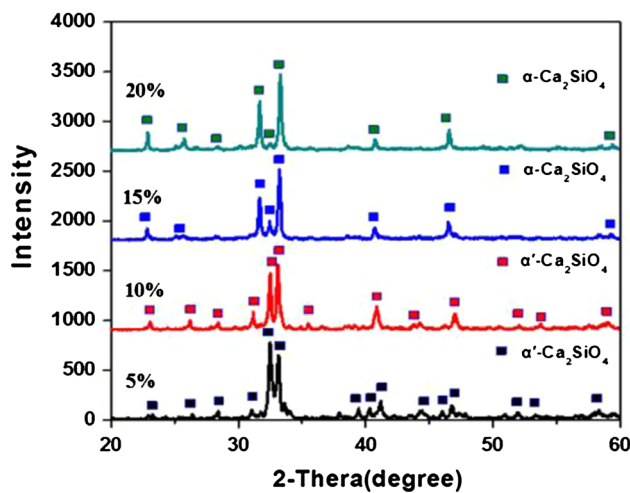


Fig. 16—X-ray diffraction of the $(2CaO \cdot SiO_2 - 3CaO \cdot P_2O_5)$ solid solution with various P_2O_5 content.

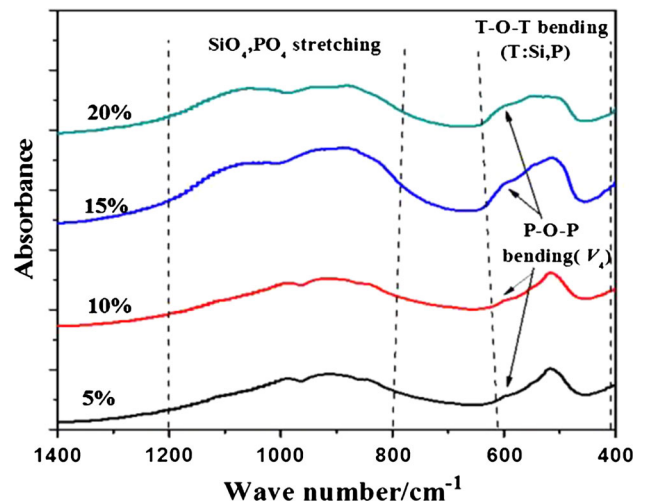


Fig. 17—Infrared spectroscopy pattern of the $(2CaO \cdot SiO_2 - 3CaO \cdot P_2O_5)$ solid solution with various P_2O_5 content.

Meanwhile, the cross section of SEM images for the above-mentioned solid solutions is presented in Figure 19, where it can be observed that with a higher P_2O_5 content, the formed solid solution is more compact and shows a smaller size. Combined with the results of density, it is consistently suggested that the $(2CaO \cdot SiO_2 - 3CaO \cdot P_2O_5)$ solid solution becomes more and more dense with the increment of P_2O_5 content.

The above results could be explained as follows: When the P_2O_5 content in the solid solution is improved, it means that the number of Si ion in the network replaced by P is increased,^[4,10] thus, the number of P-O-P bonds in the solid solution will increase accordingly. Consequently, the bending vibration (ν_4) of

P-O-P in the second band becomes obvious. In general, the phosphorus ionic (P^{5+}) radius is 0.035 nm shorter than the silicon ionic (Si^{4+}) radius of 0.039 nm,^[4] and the number of electrons outside of P is one more than that of Si; as a result, the bond length of (P-O) is shorter than that of (Si-O). Therefore, the structure of the solid solution would be changed and the density would increase with the addition of P_2O_5 content.

The present result suggested that the formed $(2CaO \cdot SiO_2 - 3CaO \cdot P_2O_5)$ solid solution layer at the edge of a large $2CaO \cdot SiO_2$ particle becomes more and more compacted as the accumulation of phosphorus concentration in the solid solution increases, which implies that the mass transfer of phosphorus from the solid solution

layer to the core of solid $2\text{CaO}\cdot\text{SiO}_2$ is very difficult. Therefore, the distribution of phosphorus concentration gradient would occur from the solid solution to the internal $2\text{CaO}\cdot\text{SiO}_2$ crystal core as shown in Figure 11. However, on the other hand, when the P_2O_5 content was increased from 3.0 mg to 6.0 mg, the concentration gradient of phosphorus became larger, leading to the change of solid solution density and structure, so the residual stress might form between the formed solid solution layer and the internal of $2\text{CaO}\cdot\text{SiO}_2$ crystal. Once the generated residual stress is high enough to

break the system's balance, the formed $(2\text{CaO}\cdot\text{SiO}_2\text{-}3\text{CaO}\cdot\text{P}_2\text{O}_5)$ solid solution reaction layer would be torn and peeled off from the surface of the $2\text{CaO}\cdot\text{SiO}_2$ particle, which seems to be able to explain the above-mentioned peeling phenomenon. Further research is needed to clarify the phenomenon in the future.

IV. CONCLUSIONS

In this article, the mass transfer behavior of phosphorus from the liquid slag phase to the solid $2\text{CaO}\cdot\text{SiO}_2$ particle in the multiphase slag at 1623 K (1350 °C) was investigated by using SHTT. The specific conclusions are summarized as follows:

1. With the addition of reagent P_2O_5 powders, the phosphorus quickly dissolves into the liquid slag and transfers from the liquid slag to the solid $2\text{CaO}\cdot\text{SiO}_2$ particle. It reacts with the external part of a solid $2\text{CaO}\cdot\text{SiO}_2$ particle to form the $(2\text{CaO}\cdot\text{SiO}_2\text{-}3\text{CaO}\cdot\text{P}_2\text{O}_5)$ solid solution.
2. Once the $(2\text{CaO}\cdot\text{SiO}_2\text{-}3\text{CaO}\cdot\text{P}_2\text{O}_5)$ solid solution is formed at the edge of the large $2\text{CaO}\cdot\text{SiO}_2$ particles, the limiting step of the further mass transfer of phosphorus is the diffusion of phosphorus through the formed $(2\text{CaO}\cdot\text{SiO}_2\text{-}3\text{CaO}\cdot\text{P}_2\text{O}_5)$ solid solution reaction layer into the internal core of the $2\text{CaO}\cdot\text{SiO}_2$ crystal.
3. When the amount of adding P_2O_5 content is increased from 3.0 to 6.0 mg, the enrichment process of phosphorus is changed. The formed $(2\text{CaO}\cdot\text{SiO}_2\text{-}3\text{CaO}\cdot\text{P}_2\text{O}_5)$ solid solution at the edge of large

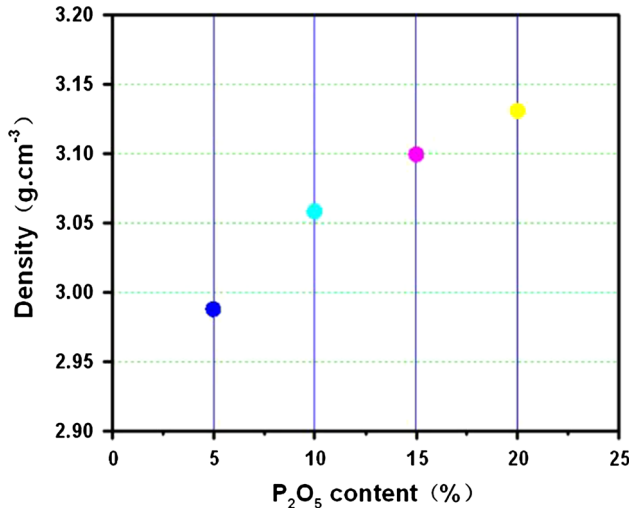


Fig. 18—Density of the $(2\text{CaO}\cdot\text{SiO}_2\text{-}3\text{CaO}\cdot\text{P}_2\text{O}_5)$ solid solution with various P_2O_5 .

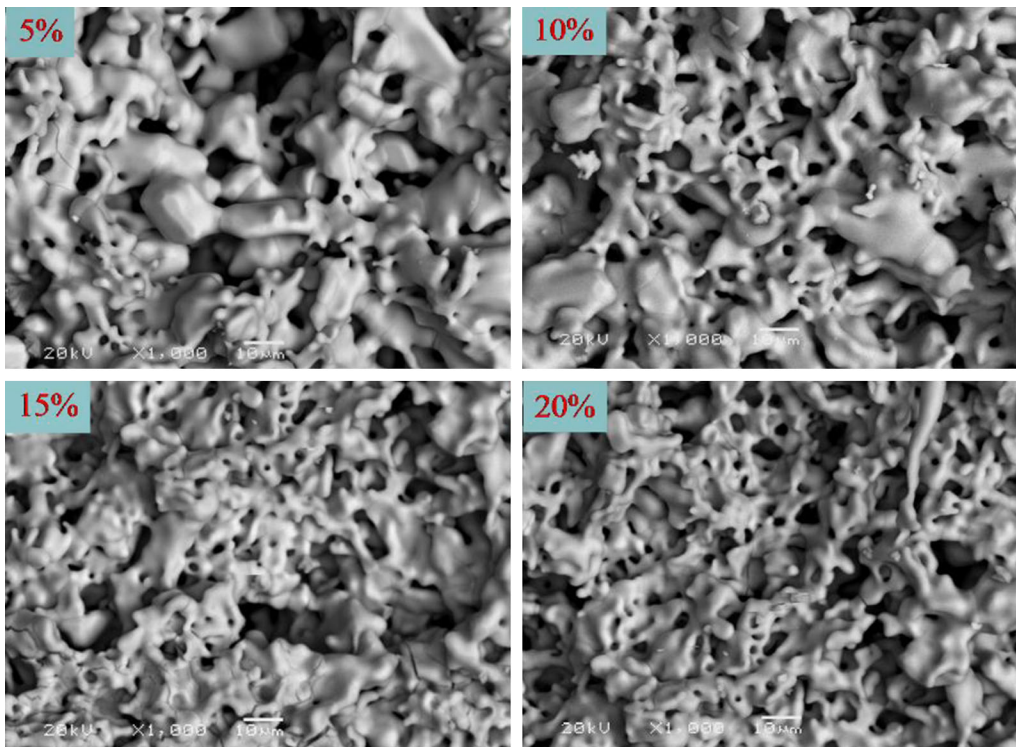


Fig. 19—SEM images of the $(2\text{CaO}\cdot\text{SiO}_2\text{-}3\text{CaO}\cdot\text{P}_2\text{O}_5)$ solid solution with various P_2O_5 content under the same magnification of 1000.

2CaO·SiO₂ particles is torn and peeled off from the surface of a solid 2CaO·SiO₂ particle.

- The study also suggests the structure of a solid solution is varied with the addition of P₂O₅ content, where the more compacted structure is formed leading to the increase in solid solution density. As a result, a mechanism of phosphorous mass transfer is proposed in that the limiting step of mass transfer of phosphorus from the solid solution layer to the core of solid 2CaO·SiO₂ is due to the compacted structure formation of a solid solution with the accumulation of phosphorous. Thus, the distribution of a phosphorous concentration gradient could occur. However, the further accumulation of phosphorous leads to the change of solid solution density and structure, so the residual stress occurs, and this may cause the formed solid solution reaction layer to tear and peel off from the large 2CaO·SiO₂ particles.

ACKNOWLEDGMENT

Financial support for the innovation-driven plan at Central South University and Hunan Excellent Young Scholar Funding (14JJ1005) is greatly acknowledged.

REFERENCES

- F. Tsukihashi: *Tetsu-to-Hagané*, 2009, vol. 95, p. 187.
- T. Hamano, S. Fukagai, and F. Tsukihashi: *ISIJ Int.*, 2006, vol. 46, pp. 490–5.
- X. Yang, H. Matsuura, and F. Tsukihashi: *ISIJ Int.*, 2009, vol. 49, pp. 1298–307.
- S. Xie, W. Wang, Y. Liu, and H. Matsuura: *ISIJ Int.*, 2014, vol. 54, pp. 766–73.
- S. Xie and W. Wang: *Steel Res. Int.*, epub ahead of print. DOI: [10.1002/srin.201400582](https://doi.org/10.1002/srin.201400582).
- S. Xie and W. Wang: *Steel Res. Int.*, epub ahead of print. DOI: [10.1002/srin.201500080](https://doi.org/10.1002/srin.201500080).
- R. Inoue and H. Suito: *ISIJ Int.*, 2006, vol. 46, pp. 188–94.
- X. Gao, M. Hiroyuki, IL Sohn, W Wang, DJ Min, and T Fumitaka: *Metall. Mater. Trans. B*, 2013, vol. 54, pp. 544–52.
- H. Takeshita, M. Hasegawa, Y. Kashiwaya, and M. Iwase: *Steel Res. Int.*, 2010, vol. 81, pp. 100–04.
- M. Hasegawa, Y. Kashiwaya, and M. Iwase: *High Temp. Mater. Process.*, 2012, vol. 31, pp. 421–26.
- W. Fix, H. Heymann, and R. Heinke: *J. Am. Ceram. Soc.*, 1969, vol. 52, pp. 346–47.
- H. Suito, Y. Hayashida, and Y. Takahashi: *Tetsu-to-Hagané*, 1977, vol. 63, pp. 1252–57.
- S. Kitamura, H. Shibata, K. Shimauchi, and S. Saito: *La Revue de Métallurgie*, 2008, vol. 105, pp. 263–71.
- K. Shimauchi, S. Kitamura, and H. Shibata: *ISIJ Int.*, 2009, vol. 49, pp. 505–11.
- R. Inoue and H. Suito: *ISIJ Int.*, 2006, vol. 46, pp. 174–79.
- I. Hoshikawa, T. Mimura, and S. Kimura: *Proc. Asia Steel Int. Conf.*, ISIJ, Tokyo, 2006, p. 454.
- S. Kitamura, S. Saito, K. Utagawa, H. Shibata, and D.G. Robertson: *ISIJ Int.*, 2009, vol. 49, pp. 1838–44.
- J. Zhou, X. Bi, and F. Yang: *Adv. Mater. Res.*, 2013, vol. 785, pp. 31–7.
- L. Zhou, W. Wang, D. Huang, J. Wei, and J. Li: *Metall. Mater. Trans. B*, 2012, vol. 43B, pp. 925–36.
- B. Lu, W. Wang, J. Li, H. Zhao, and D. Huang: *Metall. Mater. Trans. B*, 2013, vol. 44B, pp. 365–77.
- L. Zhou, W. Wang, J. Wei, and M. Jin: *ISIJ Int.*, 2013, vol. 53, pp. 665–72.
- K. Fukuda, I. Maki, S. Ito, H. Yoshida, and K. Aoki: *J. Am. Ceram. Soc.*, 1994, vol. 77, pp. 2615–19.
- M. Somerville and S. Jahanshahi: *Renew. Energ.*, 2015, vol. 80, pp. 471–8.
- R. Virtudes, A.C. Miguel, D.A. Salvador, and N.D. Piedad: *J. Am. Ceram. Soc.*, 2011, vol. 94, pp. 4459–62.
- B.O. Mysen: *Am. Mineral.*, 1990, vol. 75, p. 120.
- P. McMillan: *Am. Mineral.*, 1984, vol. 69, pp. 622–44.
- B.O. Fowler, M. Markovic, and W.E. Brown: *Chem. Mater.*, 1993, vol. 5, p. 1417.
- A. Stoch, W. Jastrzebski, A. Brozek, J. Stoch, J. Szaraniec, B. Trybalska, and G. Kmita: *J. Mol. Struct.*, 2000, vol. 555, pp. 375–82.
- H. Zeng and W.R. Lacefield: *Biomaterials*, 2000, vol. 21, pp. 23–30.
- C. Huang and E.C. Behrman: *J. Non-Cryst. Solids*, 1991, vol. 128, pp. 310–21.
- Y. Sun, K. Zheng, J. Liao, X. Wang, and Z. Zhang: *ISIJ Int.*, 2014, vol. 54, pp. 1491–7.